Evaluation of adhesively bonded composites by nondestructive techniques

Paweł H. Malinowski[1*], Romain Ecault[2], Tomasz Wandowski[1], Wiesław M. Ostachowicz[1,3]

[1] Institute of Fluid–Flow Machinery, Polish Academy of Sciences
Fiszera 14, 80-231, Gdansk, Poland

[2] Airbus Group Innovations, Campus Engineering (D42/D41),
BP90112, 31703 Blagnac, France

[3] Warsaw University of Technology, Faculty of Automotive and Construction Machinery,
84 Narbutta St., 02-524 Warsaw, Poland

Keywords: composites, CFRP, NDT, NDE, ultrasonics, electromechanical impedance, EMI, adhesive bonds

Abstract. Composite materials are commonly used in many branches of industry. One method to join or repair CFRP parts is by the use adhesive bonding. There is a search of effective methods for pre-bond assessment of bonded parts and post-bond inspection. Research reported here focuses on post-bond inspection of bonded CFRP plates. In this paper we reported results of two methods. We used noncontact ultrasonic testing (UT) technique as reference method. Ultrasonic testing was made in an immersion tank using phased-array probes. The second method was the electromechanical impedance (EMI). A piezoelectric sensors were surface mounted on each of the samples. Due to piezoelectric effect the electrical response of the sensor is related to mechanical response of the structure to which the sensors is bonded to. Measurements were conducted using HIOKI Impedance Analyzer IM3570. In order to perform a detailed study three samples of each kind were tested. There were three reference samples. The samples with modified adhesive bonds had three levels of severity, so there were three samples with each level of modification. The ultrasonic testing was focused on C-scan analysis taking into consideration the amplitude and time of flight (TOF). Two probes were used, one with 5 MHz frequency, second with 10 MHz. The EMI spectra were gathered up to 5 MHz and they were processed with signal processing algorithms in order to extract differences between reference samples and samples with modified bonds. The UT results provided relevant information about the investigated samples, while the EMI showed sensitivity to the level of adhesive bond modification.

*pmalinowski@imp.gda.pl; phone +48 58 5225 174; fax +48 58 341 61 44; www.imp.gda.pl/en/o4/z1/

Health Monitoring of Structural and Biological Systems 2017, edited by Tribikram Kundu, Proc. of SPIE
Vol. 10170, 101700B · © 2017 SPIE · CCC code: 0277-786X/17/$18 · doi: 10.1117/12.2259852

1. INTRODUCTION

Many efforts are put to the development of techniques that can ensure reliable adhesive bonds. This paper focuses on adhesive joints of CFRP part. Adhesive bonding is used both in manufacturing and in adhesively bonded patches used for repairs. It is crucial to assess the quality of such bonds. The performance of adhesive bonds depends on the state of the joint surfaces. Improper preparation of the surface before bonding may lead to weak bond. One can distinguish two branches related to reliable adhesive bonding. One is devoted to assessment of the surface quality before bonding [1]. The second one concentrates on the assessment of the bond itself [2]. Mechanical tests published in the past showed bond weaknesses related to contamination or bad curing of the adhesive [3]. Here, we use two methods of assessment. Ultrasonic testing is considered as conventional NDT (Non Destructive Testing) technique for part quality control. This technology is the most used for composite material inspection, in aeronautics, but in other domains too. It is thus considered as a standard method by end-users. In this work, ultrasonic inspections are realized in order to check the quality of the produced bonded samples. Indeed, according to literature, a "weak bond" should not be detected by conventional NDT methods. Else these bonds would be considered as bond with defects (such as voids, porosity, disbonding, etc.). Next the EMI method was used. A promising results of using it for assessment of adhesive bonds was presented in [4]. A lap joint of aluminium with a piezoelectric sensor inside was studied. For the composite adhesive bonds the method was used in [5]. In the new research presented here we used samples with different lay-up, contamination level, and adhesive in comparison to work published in [5].

2. METHODS OF ASSESSMENT

The EMI method is one of the used in this study. In the EMI method electric quantities of a piezoelectric sensor are measured. This sensor is either bonded on or embedded in an investigated object. The measurements are gathered for chosen frequency band. Due to direct and converse piezoelectric effect, the sensor excites the object and senses the response from it. This electromechanical coupling causes that the registered impedance spectra are modified by the presence of the host structure. Various structural factors have its influence on the registered spectra. Appearance of additional resonance peaks, peak shift in frequency or magnitude change can be treated as indicator of change (damage, debonding, etc.) within the object. In order to extract damage related features for the EMI spectra various frequency bands are analyzed. These bands depend on the inspected structure, the used piezoelectric sensor and the abilities of the available equipment. In this particular work we limit ourselves to 5 MHz because this is the maximal frequency achieved by our impedance analyser.

Ultrasounds inspections were performed in Airbus Group Innovations laboratory, using a 6-axis mechanics and a M2M ultrasonic generator (see Figure 1-c and b respectively). Immersion configuration has been selected to maximize the signal quality. Samples are placed by consistent group in the water tank on metal beams (see in Figure 1-d). The waterpath, meaning the distance between the probe and the samples was set to 40mm in average. Two different phased-array probes were used for inspection (see example in Figure 1-a). Characteristics are given below, with the trajectory parameters for each:

- 5MHz linear probe, 64 elements, 1.0 mm pitch, 64 mm of aperture, 10 mm elevation, flat focusing; Linear scanning; scanning step: 2mm (standards), increment 30 mm
- 10 MHz linear probe, 64 elements, 0.5 mm pitch, 32 mm of aperture, cylindrical focusing (R = 40 mm); scanning step: 1mm, increment 20 mm (i.e. 33% of overlap).

The 5MHz probe corresponds to the Airbus standards. It was important to check that it was not possible to highlight any contamination-induced defects using the current production tools. The 10 MHz probe was chosen for complementary investigations. The higher central frequency might enable further frequency analyses, and the smaller element size could be used to detect smaller defects.

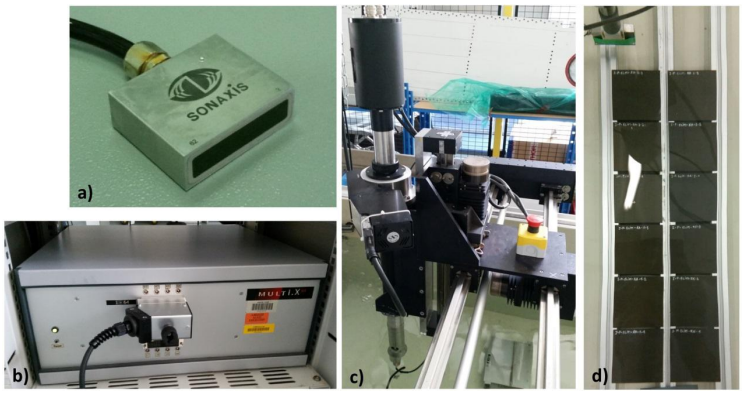

Figure 1. Overview of the ultrasonic inspection setup with a) example of a phased-array probe (64L, 5MHz); b) Ultrasounds generator for emission and reception (M2M MultiX); c) Water tank and the 6-axes mechanics to scan the parts; d) typical placement of the samples in the water tank for inspections

3. SAMPLES

The material used for samples was Hexcel M21E. The size of samples was 10 cm x 10 cm. The samples comprised of two plates adhesively bonded together with film adhesive. Each plate was made with 8 plies and layup sequence: $[0, 0, 45, -45]_S$. In total five types of samples were investigated. There were two types of reference samples. A set simulating the bonding during a production of a composite structure was denoted by PRE. The PRE samples were bonded with FM 300 K adhesive cured at 171˚C. A set simulating the bonding process during a repair of composite structure was denoted by RRE. The RRE samples were bonded with FM 300-2 adhesive cured at 121˚C. The production-related bond modification was based on contamination with silicon-based release agent (sample symbol: PRA). It was applied in three defined concentrations on clean CFRP plates by means of dip-coating. The indicator of contamination level was based on silicon concentration on the contaminated surface. The repair-related bond modification was based on thermal treatment of the samples (RTD samples) and pre-curing (RFC samples). Three RTD samples were prepared for each of the three levels of temperature. There were three RFC samples prepared by local pre-curing of adhesive before the bonding process. All the investigated sample types and symbols were gathered in Table 1.

Table 1. Investigated samples; assigned symbols and description

Symbol	Description
PRE1, PRE2, PRE3, RRE1, RRE2, RRE3	Reference samples with unmodified bond, P –production scenario samples, R – repair scenario samples
PRA11, PRA12, PRA13	Pre-bond contamination with release agent, level 1 – 3.2 at.% of Si
PRA21, PRA22, PRA23	Pre-bond contamination with release agent, level 2 – 5.1 at.% of Si
PRA31, PRA32, PRA33	Pre-bond contamination with release agent, level 3 – 6.2 at.% of Si
RTD11, RTD1112, RTD1113	Pre-bond thermal treatment, level 1 – 220˚C
RTD1121, RTD1122, RTD1123	Pre-bond thermal treatment, level 2 – 260˚C
RTD1131, RTD1132, RTD1133	Pre-bond thermal treatment, level 3 – 280˚C
RFC11, RFC12, RFC13	Pre-curing of adhesive, high level
RFC21, RFC22, RFC23, RFC31, RFC32, RFC33	Pre-curing of adhesive, low level

4. ULTRASONIC RESULTS

In order to display ultrasonic results, software settings (or gates) are necessary. Typical B-scan and A-scan are given in Figure 2a with the gate display on it. Main echoes can be observed: 1. Front wall echo (FWE), 2. Bond echo (Bond), 3. Back Wall Echo (BWE). All the gates are synchronized using a synchronization gate tracking the entry echo. Theses

gates can then be used for the analysis. “FWE_max” gets the maximum of the front wall echo. It can be used to check the acquisition quality, and highlight surface defects, “g+” records the maximum echo after FWE. Typically, bond or back wall in this case. Particularly useful to compare the echoes, “Bond” is centered on the bond echo and tracks its maximum, “BWE” is centered on the BWE and tracks its maximum

These gates are used to generate cartographies, also called C-scan, where the amplitude (%) or the time-of-flight (TOF) of the recorded echo is displayed in the inspection plan (see an amplitude cartography example in Figure 2b. Samples are always placed the same way, references on the bottom right, other samples around them. For each sample, origin is taken on the top left corner for defect positioning.

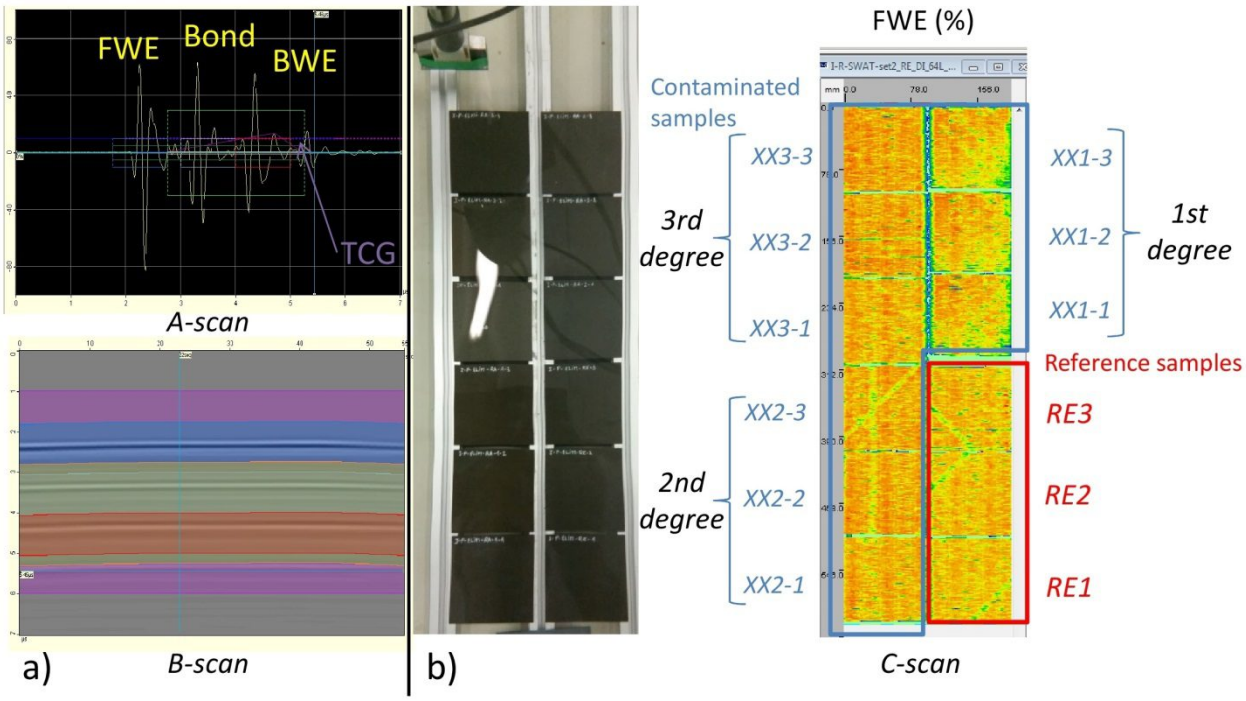

Figure 2. Example of the results, a) Typical A-scan and B-scan with gates setting display, b) example of cartographies in amplitude for bonded coupons, with the corresponding sample positions

Inspection results are presented in Figure 3 to Figure 5 for PRA samples, RTD samples, and RFC samples, respectively. Ultrasound signals are given as cartographies or C-scan for different gate using amplitude or time of flight. The analysis of these cartographies enables to highlight two different defect types for the investigated samples. The manufacturing defect have low impact on the evaluation of the bonds. There is bending, particularly observed for RRE samples. The curvature is seen on the FWE_max amplitude cartography, with the 5 MHz probe, as shown in Figure 5. The observed amplitude gradient is typical from a probe misalignment with the specimen, thus of a bending. It could also be a bad surface quality. The second type is related to bond modification. These are defects such as disbonding or delamination (in the case of RFC and RTD samples). Results are given in Figure 4 and Figure 5. In RTD31 sample, an important delamination is highlighted by ultrasonic inspections (see in Figure 4), on the top left corner. The delamination is evidenced using all the gates because it is located on the first composite skin, i.e. the one which has been thermally affected. This is confirmed by the g+ TOF cartography (dark blue). Therefore, the defect has consequences on all the other gates. In FC1 samples, disbondings are evidenced in the middle of each plate. Defect signature is visible on the bond amplitude and TOF cartographies. Highest amplitude and small shift in TOF respectively show the disbondings. Defects are consequently visible on the BWE amplitude gate with a low amplitude region, and on the g+ TOF cartography. These disbondings are located in the middle of the bonded coupons, and can thus have an important impact on other measurements. Note that some small disbondings (below 1 cm) were also observed in some of the FC-2 samples. Sizes of the disbondings have been estimated using the “defect detection” tool of the analysis software

(NDTKit). Results are presented in Figure 6, with their main characteristics: position in the plate, surface, outline surface, length and mean value (for TOF). The origin is taken for each plate at the top left corner for the defect position.

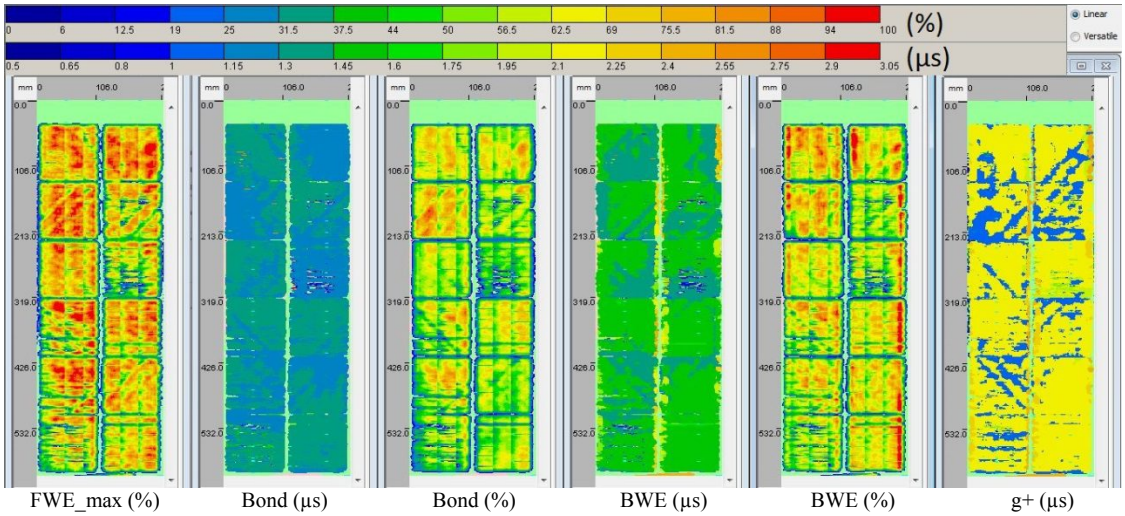

FWE_max (%) Bond (µs) Bond (%) BWE (µs) BWE (%) g+ (µs)

Figure 3. 5MHz inspection results for PRE and PRA samples

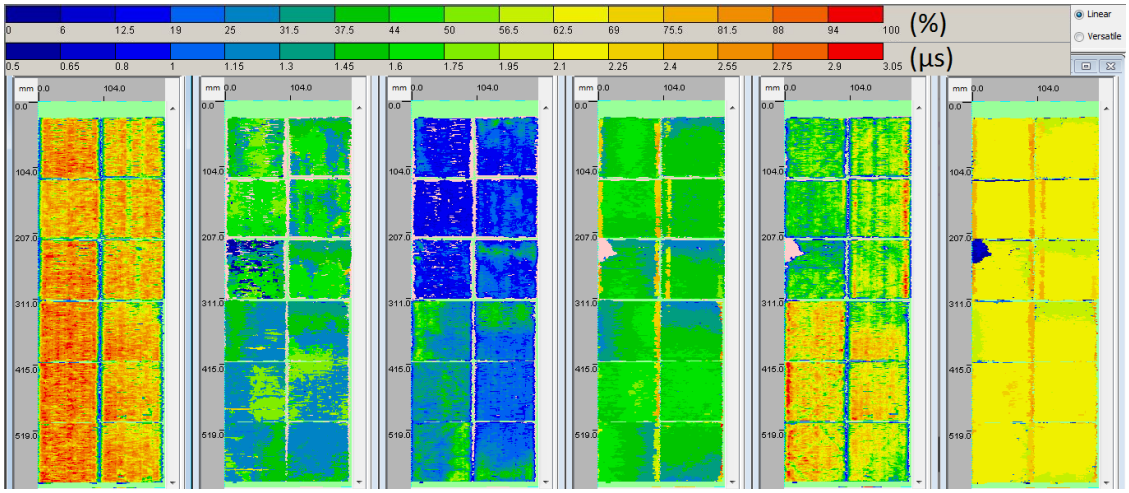

FWE_max (%) Bond (µs) Bond (%) BWE (µs) BWE (%) g+ (µs)

Figure 4: 10MHz inspection results for RRE and RTD samples

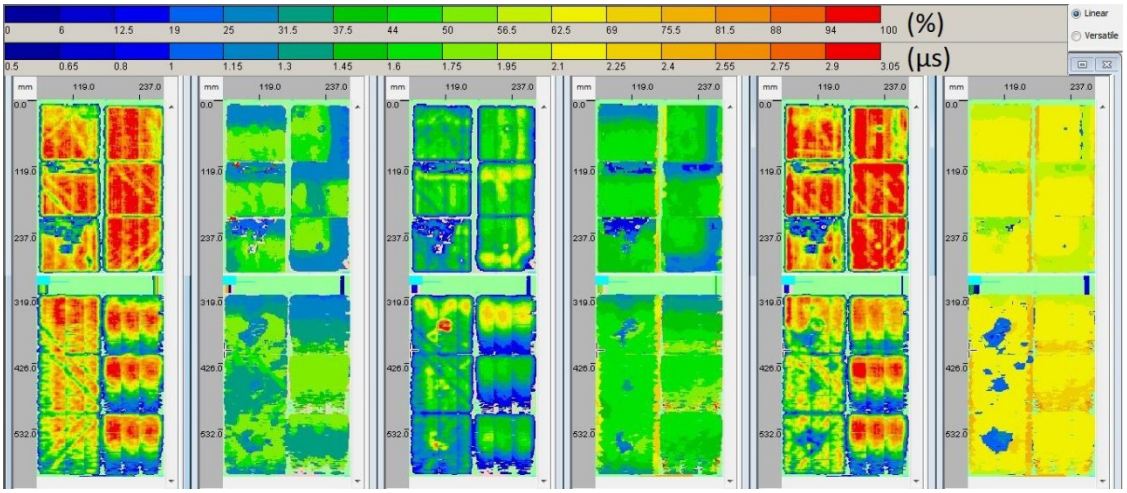

Figure 5: 5MHz inspection results for RRE and RFC samples

Defect Detection	Names (centers)	Area (mm²)	Outline (mm²)	Length (mm)	Mean (µs)
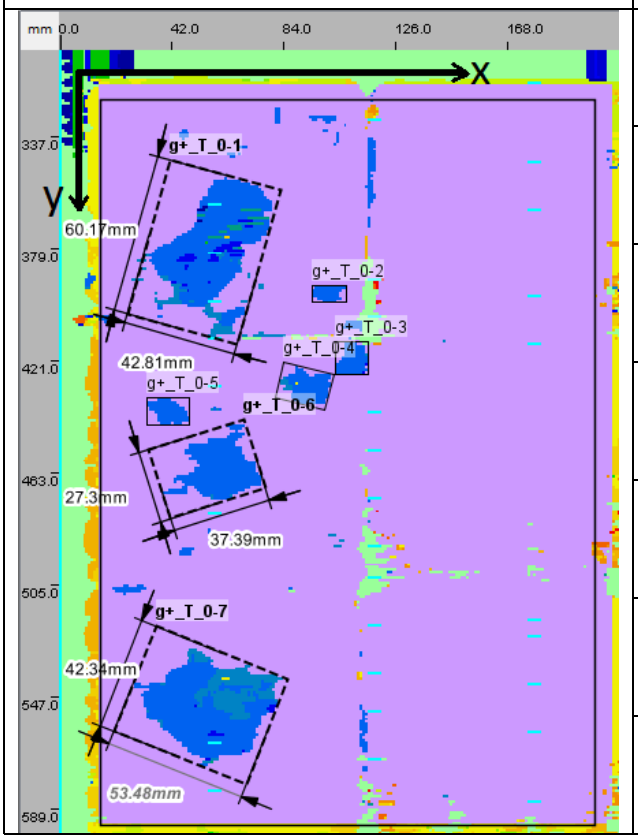	g+_T_0-1 (X=43, Y=62)	1328.0	2575.6	60.2	1.08
	g+_T_0-2 (X=92, Y=81)	57.0	78.0	13.0	1.08
	g+_T_0-3 (X=98, Y=7)	115.0	144.0	12.0	1.09
	g+_T_0-4 (X=80, Y=20)	174.0	260.2	19.2	1.12
	g+_T_0-5 (X=28, Y=27)	108.0	160.0	16.0	1.08
	g+_T_0-6 (X=49, Y=49)	517.0	1020.9	37.4	1.07
	g+_T_0-7 (X=44, Y=44)	1350.0	2264.3	53.5	1.12

Figure 6: Defect size estimation for RFC11, RFC12 and RFC13 samples

5. EMI RESULTS

Following the previous investigations the EMI conductance (G) spectra were assessed in the 3-5 MHz band. In order to compare the conductance characteristics the RMSD index was used:

$$RMSD = \sqrt{\frac{\sum_i \left(G_i - G_i^r\right)^2}{\sum_i \left(G_i^r\right)^2}} \times 100\% \quad (1)$$

The r-subscript represents the reference conductance. During the ultrasonic inspection there were no indications for the PRA samples, so it was assumed that the samples at each level of contamination are similar and their spectra were averaged. However, the samples with following symbols: PRE3, PRA12 and PRA23 were not taken into consideration. The spectra for mentioned samples looked differently perhaps due to wrong bonding or damage to the sensor. The average spectra calculated for PRE1 and PRE2 samples were taken as reference in calculating the RMSD index. The results for the release agent contaminated samples are presented in Figure 7a). An increase in the difference between the spectra is observed as the bond line contamination increase. In the case of thermally treated samples the ultrasonic testing indicated the only one sample differs from the rest. Sample RTD31 had a delamination, most probably caused by the heating. For this reason the results for the highest level of thermal treatment (280^{o}C) were not averaged but separated. Moreover, also in this set of samples some of the spectra differ for unknown reason. Following results were rejected from analysis: RRE2, RTD12, RTD22, RTD33. The results for RTD samples are presented in Figure 7b). The difference from the reference set increases with the increasing temperature of treatment. Moreover, the highest value for RMSD is obtained for RTD31 for which the delamination was observed.

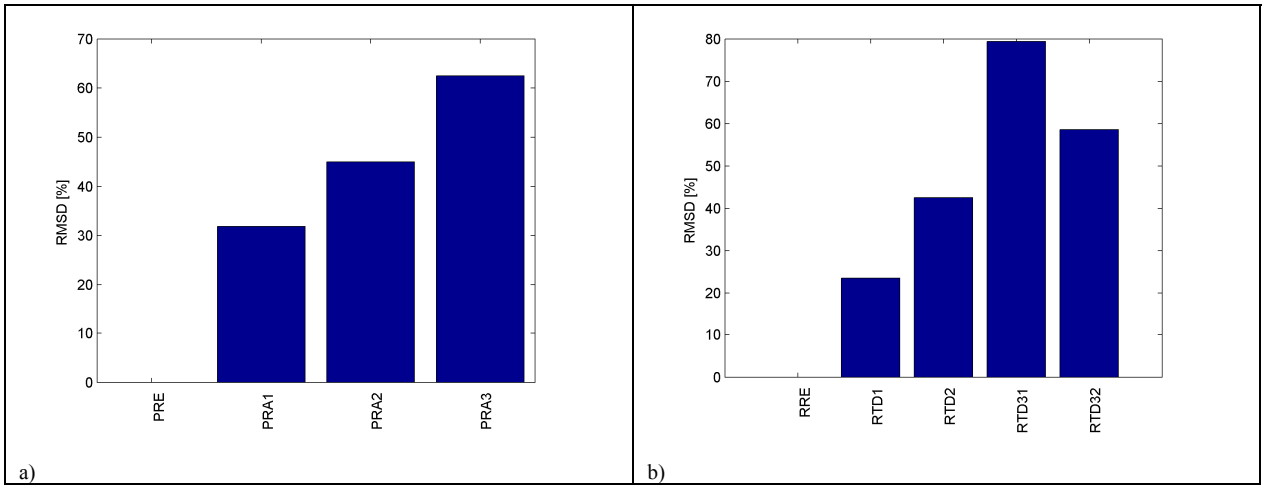

Figure 7: RMSD values for PRA (a) and RTD (b) sets of samples

The last case is more complicated because the three samples that had pre-cured adhesive showed a disbonding areas at the bond line. This samples were denoted by RFC11, RFC12 and RFC13. The size and shape of this disbondings were different between samples as it was shown in Figure 6. In order to assess the influence of this bonds of the conductance spectra the maximum of the conductance was tracked. The first index defined as

$$\Delta f = \frac{f - f_p}{f_p} \times 100\% \quad (2)$$

tracked changes of the frequency of maximum (*f)* for the conductance curve in relation to the frequency of this maximum f_p for the piezoelectric sensor before bonding. The second index tracked the change of the value of this maximum (*M*) in relation to the unbonded sensor (M_P). The index was defined as follows:

$$\Delta M = \left| \frac{M - M_p}{M_p} \right| \times 100\% \tag{3}$$

Results are depicted in Figure 8. One can notice that highest values are obtained for RFC11. The second highest value if observed for RFC13 sample. As was shown in Figure 6 these two samples have the largest area of the disbond. The values of *Δf* and *ΔM* were compared against the disband area estimated from the ultrasonic testing. The result of this comparison is shown in Figure 9.

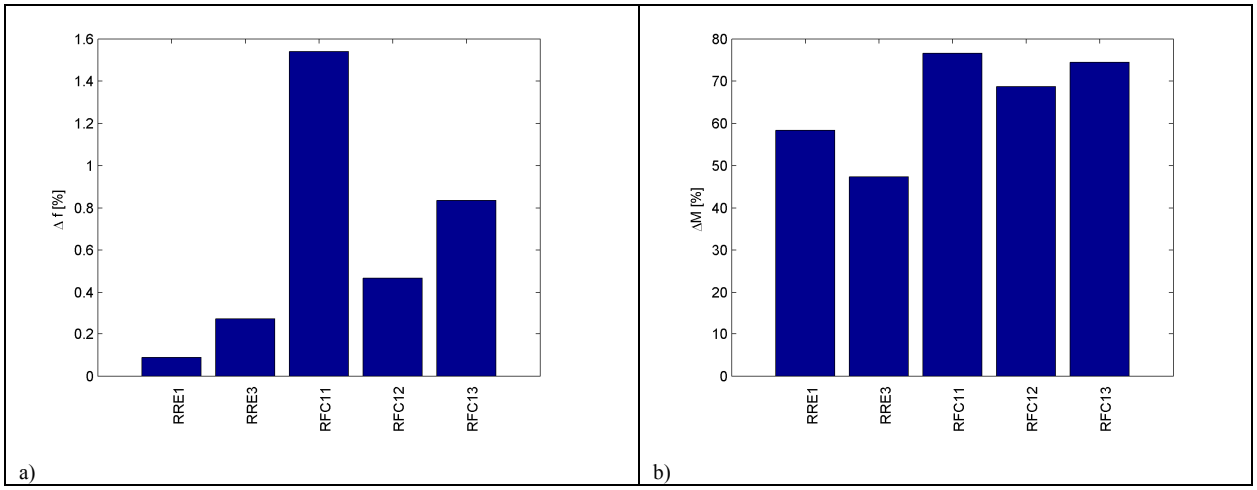

Figure 8: The change of conductance maximum for RFC samples in relation to unbonded sensors; a) – frequency shift, b) – maximum peak height

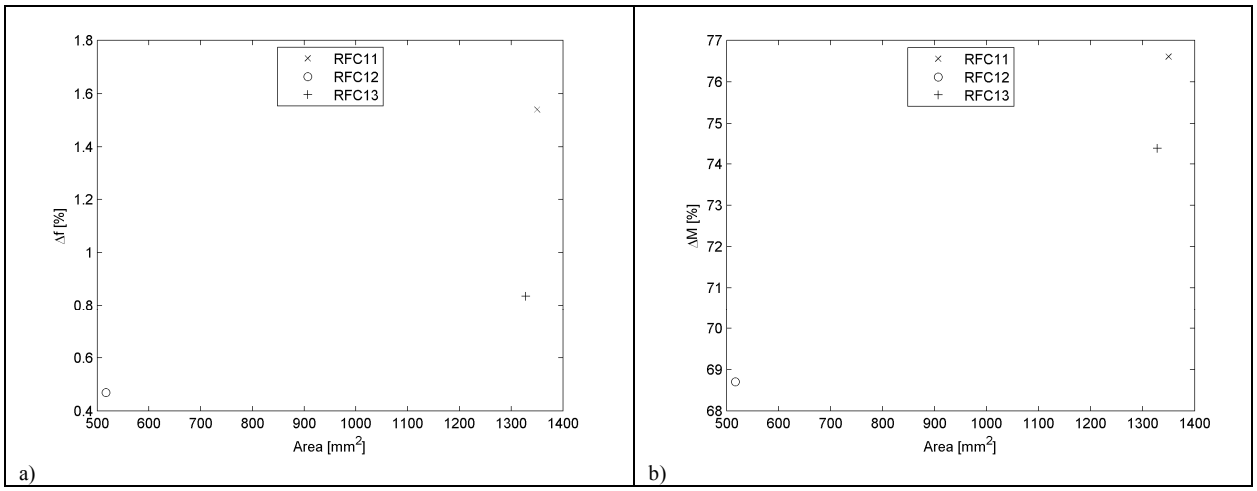

Figure 9: Relation of *Δf* and *ΔM* to the area of detected disbands for FC1 samples; a) – frequency shift, b) – maximum peak height

6. CONCLUSIONS

In this paper, the conventional ultrasonic inspections of contaminated bonded samples were presented and detailed. Objective was to state on the specimen quality, and on the weak bond status. All the samples were investigated using two different probes (5MHz and 10 MHz). For these samples, two different kinds of defects were observed. Manufacturing defect with low impact such as bending, surface quality problem. Treatment induced defects such as disbonding (RFC1 samples) or delamination (RTD31 sample). After the ultrasonic testing the EMI method was used. It was shown that the increasing level of contamination can be correlated with the RMSD value calculated for the conductance curves. The index for RTD31 with delamination also differs from the remaining cases that were

considered. The disbonds caused by pre-curing of the adhesive (RFC1 samples) correlate with the change of the maximum conductance peak location and its value.
The research is continued. Other type of modified bonds related to production or repair process are investigated. Comparison with results of the mechanical tests is also foreseen.

ACKNOWLEDGMENTS

The research leading to these results has been partially supported by project funded by Polish National Science Center under the decision no. DEC-2013/11/D/ST8/03355. This project has received funding from the European Union's Horizon 2020 research and innovation programme under grant agreement no 636494.

REFERENCES

[1] Brune, K., Lima, L., Noeske, M. et al. "Pre-bond Quality Assurance of CFRP Surfaces Using Optically Stimulated Electron Emission," Proc. 3rd International Conference of Engineering Against Failure (ICEAF III) 26-28 June, Kos, Greece, 300-307 (2013).
[2] Markatos, D.N., Tserpes, K.I., Rau, E. et al. "Degradation of Mode-I fracture toughness of CFRP bonded joints due to moisture and release agent and moisture pre-bond contamination," Journal of Adhesion 90, 156-173 (2014).
[3] Markatos, D.N., Tserpes, K.I., Rau, E. et al. "The effects of manufacturing-induced and in-service related bonding quality reduction on the mode-I fracture toughness of composite bonded joints for aeronautical use," Composites: Part B 45, 556–564 (2013).
[4] Dugnani, R., Zhuang, Y., Kopsaftopoulos, F., Chang, F.-K., "Adhesive bond-line degradation detection via a cross-correlation electromechanical impedance–based approach," Structural Health Monitoring 15(6), 650-667 (2016).
[5] Malinowski, P., Wandowski, T., Ostachowicz, W., "The use of electromechanical impedance conductance signatures for detection of weak adhesive bonds of carbon fibre–reinforced polymer," Structural Health Monitoring 14(4), 332-344 (2015).